Chemosphere 159 (2016) 80–88

Contents lists available at ScienceDirect

Chemosphere

journal homepage: www.elsevier.com/locate/chemosphere

Ultrasensitive detection of inhaled organic aerosol particles by accelerator mass spectrometry

E.V. Parkhomchuk [a, b, *], D.G. Gulevich [a, b], A.I. Taratayko [a, c], A.M. Baklanov [d], A.V. Selivanova [a, e], T.A. Trubitsyna [e], I.V. Voronova [a], P.N. Kalinkin [a, b], A.G. Okunev [a, b], S.A. Rastigeev [a, f], V.A. Reznikov [a, c], V.S. Semeykina [a, b], K.A. Sashkina [a, b], V.V. Parkhomchuk [a, f]

[a] Novosibirsk State University, Laboratory of Radiocarbon Methods of Analyses, 2 Pirogova st., Novosibirsk, 630090, Russia
[b] Boreskov Institute of Catalysis SB RAS, 5 Lavrentieva st., Novosibirsk, 630090, Russia
[c] N.N. Vorozhtsov Novosibirsk Institute of Organic Chemistry SB RAS, 9 Lavrentieva st., Novosibirsk, 630090, Russia
[d] Voevodsky Institute of Chemical Kinetics and Combustion SB RAS, 3 Institutskaya st., Novosibirsk, 630090, Russia
[e] JSC Tion, 20 Injenernaya str., 630090, Novosibirsk, Russia
[f] Budker Institute of Nuclear Physics SB RAS, 11 Lavrentieva st., Novosibirsk 630090, Russia

HIGHLIGHTS

- Radiocarbon labeled styrene was synthesized in five stages from ^{14}C-methanol.
- PS beads 225 ± 25 nm in size containing radiocarbon ^{14}C label were used as a model system for organic aerosol.
- Low-concentrated 10^{-3} cm^{-3} ^{14}C-aerosol was inhaled by mice during 5 days 30 min a day.
- The isotope analysis of biological probes was conducted by accelerator mass-spectrometry.
- The particle matter was directly registered in mice lungs, liver, kidneys and brain.

GRAPHICAL ABSTRACT

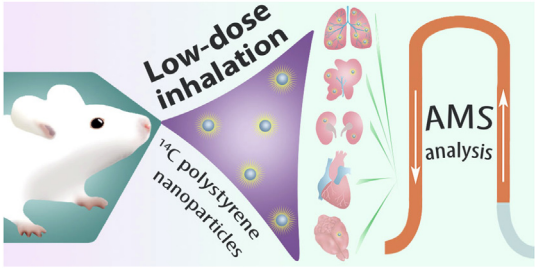

ARTICLE INFO

Article history:
Received 15 March 2016
Received in revised form
25 May 2016
Accepted 27 May 2016
Available online 6 June 2016

Handling Editor: Ralf Ebinghaus

Keywords:
Organic aerosols
Low-dose inhalation

ABSTRACT

Accelerator mass spectrometry (AMS) was shown to be applicable for studying the penetration of organic aerosols, inhaled by laboratory mice at ultra-low concentration ca. 10^3 cm^{-3}. We synthesized polystyrene (PS) beads, composed of radiocarbon-labeled styrene, for testing them as model organic aerosols. As a source of radiocarbon we used methyl alcohol with radioactivity. Radiolabeled polystyrene beads were obtained by emulsifier-free emulsion polymerization of synthesized ^{14}C-styrene initiated by $K_2S_2O_8$ in aqueous media. Aerosol particles were produced by pneumatic spraying of diluted ^{14}C-PS latex. Mice inhaled ^{14}C-PS aerosol consisting of the mix of 10^3 225-nm particles per 1 cm^3 and $5 \cdot 10^3$ 25-nm particles per 1 cm^3 for 30 min every day during five days. Several millions of 225-nm particles deposited in the

* Corresponding author. Boreskov Institute of Catalysis SB RAS, 5 Lavrentieva st., Novosibirsk 630090, Russia.
E-mail address: ekaterina@catalysis.ru (E.V. Parkhomchuk).

http://dx.doi.org/10.1016/j.chemosphere.2016.05.078

Polystyrene beads
Radiocarbon
Accelerator mass-spectrometry
Mice

lungs and slowly excreted from them during two weeks of postexposure. Penetration of particles matter was also observed for liver, kidneys and brain, but not for a heart.

1. Introduction

Human exposure to particulate matter (PM) has increased dramatically over the last century due to anthropogenic impact, including sharply grown combustion of fuels, developing road industry as well as thriving nanotechnologies (Oberdörster et al., 2005). A significant positive association between morbidity and nonaccidental mortality and air pollution by ultrafine(<0.1 μm in diameter), fine (from 0.1 to 2.5 μm) and course (more than 2.5 μm) particles has been indicated by many representative reports (Oberdörster et al., 2005; Pope et al., 1992; Dockery et al., 1992; Samet et al., 2000; Künzli et al., 2000; Peters et al., 1997a; Pope and Dockery, 2006). Such air pollutant as PM is believed to increase respiratory symptoms and illness, asthma exacerbations and chronic lung and heart disease (Bascom et al., 1996). PM is estimated to kill more than 500,000 people each year (Nel, 2005) or even more with predominant burden occurring in developing Asian countries (Cohen et al., 2005). The situation concerns not only adults but also children (Pope et al., 1992; Nel, 2005; Dockery et al., 1989), effected by both outdoor and indoor air (Jones, 1999; Wallace, 1996).

It has been shown that when inhaled, specific sizes of nanoparticles are deposited by three basic mechanisms: inertial impaction, sedimentation and diffusion, in all regions of the respiratory tract but with different efficiency. Less than 20% of fine particles and up to 90% of ultrafine particles deposit in the respiratory tract (Oberdörster, 2001a; Khorasanizade et al., 2011; Williams et al., 2011). After the deposition the alveolar-airway barrier allows passage of particles up to nearly 800 nm in diameter (Conhaim et al., 1988). Ultrafine particles are primarily consumed by interstitial macrophages (Donaldson et al., 1998) and unphagocytosed particles penetrate across epithelial and endothelial cells to the blood and lymph circulation and reach bone marrow, lymph nodes, spleen, and heart (Oberdörster et al., 2005; Oberdörster, 2001a). Access to the central nervous system and ganglia via translocation along of neurons has also been observed (Oberdörster et al., 2005). Ultrafine particles and, to a lesser extent, fine particles, localize in mitochondria, where they induce major structural damage, contributing to oxidative stress (Li et al., 2003).

Despite substantial findings regarding PM exposure-response function there are some important gaps and skepticism regarding “what we may think we know about the health effects of PM exposure”. (Pope and Dockery, 2006; Lumley and Sheppard, 2003). On the other hand, reliable studies on particle deposition in the respiratory tract and further particle translocation are of great value, not only to risk assessment of inhalation toxicology but also to improve efficiency in drug delivery of inhalation therapies (Williams et al., 2011; Miller et al., 1979). The problem of investigations on health effects of PM exposure is resulted from three main features of PM.

The first one is that health impacts from PM exposure with different particle size are unequal. Particles with different sizes from nm to μm represent separate classes of pollutants and have been recommended to be measured separately in aerosol research and medical studies (Wilson and Suh, 1997; Schwartz et al., 1996; Peters et al., 1997b). The second feature is low particle concentration of ambient aerosol. The relationship between air PM pollution and health was clearly observed at particle concentrations <100 μg m^{-3} (Dockery et al., 1992; Pope and Dockery, 2006), an excess risk of death of 0.5% per each 10 μg m^{-3} of PM_{10} (<10 μm in diameter) being observed from 5 to 220 μg m^{-3} (Schwartz, 1994; Brunekreef and Holgate, 2002). According to the U.S. Environmental Protection Agency, the 24-h and annual standards for $PM_{2.5}$ are 65 and 15 μg m^{-3}, respectively, and for PM_{10} they are 150 and 50 μg m^{-3}, respectively. (Ware, 2000; Bernstein et al., 2004). What is more, the levels of ultrafine particles in urban air are generally between 0.8 and 2 μg m^{-3}, or $1–5{\cdot}10^4$ cm^{-3} and only during episodic increases mass concentrations can rise to 20–50 μg m^{-3} with number concentrations rising to levels of $0.3–1{\cdot}10^6$ cm^{-3}. (Conhaim et al., 1988; Oberdörster, 2001a; Oberdörster et al., 2002a). Unlike direct measurement of PM concentration in air which is carried out with sufficient accuracy, the particle content in the tissues and organs after inhalation under the ambient conditions is extremely complicated. The third feature of PM is the predominantly organic nature of particles, mainly derived from mobile and stationary combustion processes. The smaller the particle size, the greater portion of particles consisting of organic substances, particles less than 200 nm in diameter being almost completely composed of organics (Mauderly and Chow, 2008). It should be noted that organic speciation of carboneous compounds in air, including PM constituents, presents a range of water-soluble (humic-like substances, polyols, polyethers, mono- and dicarboxylic acids etc.) and water-insoluble organic carbon (n-alkanes, n is from 14 to 42, n-alkanoic acids, polycyclic aromatic hydrocarbons, soot etc.), the last one often giving the higher contribution (Mauderly and Chow, 2008).

PM characteristics described above, namely ultra-small size, ultra-low concentrations and carboneous content of the aerosol have made direct detection of particles inhaled under natural conditions impossible to date. Due to strong analytical limitations the majority of PM health effect investigations are based on techniques that use intratracheal instillation instead of inhalation, and even when inhalation takes place, PM concentrations are much greater than 100 μg m^{-3} (Table 1) (Glover et al., 2008; Nemmar et al., 2001, 2002a; Takenaka et al., 2001; Oberdörster, 2001b; Ferin et al., 1992; Oberdorster et al., 1994; Geiser et al., 2005; Oberdörster et al., 2002b, 2004, 1992; Simon et al., 1995a; Simon et al., 1995b; Ercan et al., 1991; Gibaud et al., 1996; Nemmar et al., 2002b, 2003; Hamoir et al., 2003; Silva et al., 2005; Kato et al., 2003; Gibaud et al., 1994, 1998). In Table 1 we tried to summarize available data on the detection studies of model aerosols in living organisms showing the main problems of particle detection which force the researchers to use high particle doses or inadequate injection routes.

In order to detect particles directly in organs after inhalation, e.g. by elemental analyses, investigators have to use inorganic particle matter, such as Pt (Oberdörster, 2001a), Ag (Takenaka et al., 2001), and TiO_2 (Geiser et al., 2005) or radioactive labels, e.g. ^{99m}Tc (Glover et al., 2008; Nemmar et al., 2001, 2002a), physically attached to the particles (Table 1). In addition to inorganic matter, which differs from the ambient aerosol constituents, it cannot be excluded that in vivo dissolution and transport of the dissolved metals and labels were significant factors during particle detection (Oberdörster et al., 2002a). Another difficulty is a great dose of

Table 1
Experimental investigations on particles penetration and propagation following in vivo exposure.

PM	Particle size	Exposure, testee	Concentration/amount/rad.dose	Detection method	Ref.
^{99m}Tc-DTPA mannitol	2.7 μm, 3.6 μm, 5.4 μm	Inhalation, 8 healthy human	20 mg containing 20–30 MBq	Single photon emission tomography	(Glover et al., 2008)
^{99m}Tc albumin	<80 nm	Intratracheal instillation, hamsters	100 μg	Thin-layer chromatography + gamma-counter	(Nemmar et al., 2001)
^{99m}Tc- carbon	5-10 nm	Inhalation, 5 healthy human	100 MBq	Thin layer chromatography + gamma counter	(Nemmar et al., 2002a)
Ag	15 nm	6 hr-inhalation, rats, intratracheal instillation, rats	133 μg m^{-3}, or 3 × 10^6 cm^{-3} 7 μg $AgNO_3$ (4.4 μg Ag) 50 μg Ag	Inductively coupled plasma mass spectrometry analysis	(Takenaka et al., 2001)
Pt	18 nm	6 hr-inhalation, rats	110 μg m^{-3}	Inductively coupled plasma mass spectrometry analysis	(Oberdörster, 2001a)
TiO_2	12 nm 21 nm 230 nm 250 nm	6 h/day, 5 days/wk for up to 12 wk- inhalation, intratracheal instillation, rats	23 mg m^{-3} 500 μg	Current plasma atomic emission spectroscopy for TiO_2, light and transmission electron microscopy for evaluating epithelial and interstitial responses	(Ferin et al., 1992)
TiO_2	20 nm 250 nm	6 h/day, 5 days/week for 12 weeks- inhalation, rats	23 mg m^{-3}	Current plasma atomic emission spectroscopy for TiO_2, light and transmission electron microscopy for evaluating epithelial and interstitial responses	(Oberdorster et al., 1994)
TiO_2	22 nm	Inhalation, rats	$7.3 \cdot 10^6$ cm^{-3} 0.11 mg m^{-3}	Energy-filtering transmission electron microscopy	(Geiser et al., 2005)
^{13}C-graphite	20-29 nm	6 h-inhalation, 344 rats	180 μg m^{-3} 80 μg m^{-3}	^{13}C continuous-flow mass spectrometry	(Oberdörster et al., 2002b)
^{13}C-graphite	<100 nm	6 h-inhalation, 344 rats	160 μg m^{-3}	^{13}C continuous-flow mass spectrometry	(Oberdörster et al., 2004)
^{141}Ce-PS ^{95}Nb-PS	3.3 μm 10.3 μm	Intratracheal instillation, 344 rats	10, 40, 100 μg	External counting, scanning electron and optical microscopy	(Oberdörster et al., 1992)
^{14}C-amino-PS	100, 240, 470, 750, 1000 nm	Intravenous injection, mice	$4.01 \cdot 10^{11}$–$3.37 \cdot 10^9$	Liquid scintillation counting	(Simon et al., 1995a)
^{14}C-protein A-PS	240 nm	Intravenous injection, mice	$2.19 \cdot 10^{11}$	Liquid scintillation counting	(Simon et al., 1995b)
^{99m}Tc-PS-DMAEA	1-10 μm	Oral administration by rabbits and human	2.5 mg, 37 MBq for rabbits 5 mg, 74 MBq for human	Γ-camera, light microscopy	(Ercan et al., 1991)
Doxorubicin-Poly(isohexyl cyanoacrylate) Doxorubicin-PS	240 nm 201 nm	Intravenous administration, mice	15 mg kg^{-1}, 36 mg kg^{-1}, 146 mg kg^{-1}	Fluorescence microscopic examination	(Gibaud et al., 1996)
Doxorubicin-polyalkylcyanoacrylate	235, 240 nm	Intravenous administration, mice	11 mg kg^{-1}	Myelosuppressive effects; the number of granulocyte progenitors	(Gibaud et al., 1994)
Polyalkylcyanoacrylate- glycoprotein	~200 nm	Intravenously injected	300 mg kg^{-1}	Glycoprotein by HPLC	(Gibaud et al., 1998)
PS, PS-COOH,	60 nm	Intravenous injection, hamsters Intratracheal instillation, hamsters	50,100,500,5000 μg kg^{-1} 25, 50, 100 μg kg^{-1}	Biomarkers – thrombus formation, platelet aggregation Biomarkers – thrombus formation, platelet aggregation	(Nemmar et al., 2002b)
PS-NH_2	60, 400 nm	Intratracheal instillation, hamsters	5, 50, 500 μg per animal	Biomarkers -bronchoalveolar lavage (BAL) indices and peripheral thrombosis	(Nemmar et al., 2003)
	24, 110, 190 nm	Intratracheal, rabbits	$5.2 \cdot 10^{12}$–$5.2 \cdot 10^{14}$ 4 mg	Biomarkers – pulmonary microvascular permeability	(Hamoir et al., 2003)
Rose Bengal + PS	60 nm	Intraperitoneal, intravenous bolus, intratracheally instilled, rodents	0.5 mg kg^{-1}	Biomarkers – thrombogenic effects	(Silva et al., 2005)
PS Lecithin-PS	240 nm	Intratracheally instillation, rats	5 mL 0.2% suspension	Electron microscope	(Kato et al., 2003)
^{14}C-PS	225 nm 25 nm	30 min-inhalation a day during 5 days, mice	10^3 cm^{-3} or 6 μg m^{-3} $5 \cdot 10^3$ cm^{-3} or 40 ng m^{-3}	Accelerator mass-spectrometer	This work

radioactivity, when labeling the inorganic or organic (Ferin et al., 1992; Ercan et al., 1991), particles, varying from 20 to 100 MBq per testee (Table 1). This dose is several orders of magnitude higher than ambient radioactivity and requires special working conditions and license for experiments.

Polymeric monodisperse beads seem to be prospective model for aerosol investigations due to the following properties: organic matter, low biodegradability, controllable size from several nm to several μm, possibility of surface modification by negative (−COOH) or positive ($-NH_2$) functional groups, as well as by designing core-shell structures with desirable chemistry. The attraction of polymeric beads, predominantly polystyrene (PS) ones, affects the number of studies using this technique (Table 1) (Oberdörster et al., 1992; Simon et al., 1995a, 1995b; Ercan et al., 1991; Gibaud et al., 1996; Nemmar et al., 2002b, 2003; Hamoir et al., 2003; Silva et al., 2005; Kato et al., 2003; Gibaud et al., 1994, 1998), but again there are some problems in particle registration. When the direct method is used for particle detection, for example, different kinds of microscopy, one has to raise the dose so that intratracheal instillation or intravenous administration is used instead of inhalation (Table 1). As a result there is a critical gap of low doses – response relationships that urgently needs to be filled for revealing human or environmental safety exposure levels of nanoparticles (Oberdörster et al., 2005).

The present work is aimed to show the prospectives of a simple way for organic particle detection at ultra-small doses of short-duration inhalation that most closely reflect the ambient exposure levels. We used polystyrene beads that were synthesized from styrene labeled with ^{14}C. This carbon isotope is often used for labeling the functional groups of PS, resulted in the low label concentration related to PS mass and in the necessity to use high doses of particles since the detection is usually carried out by scintillation counting (Oberdörster et al., 1992; Simon et al., 1995a, 1995b; Ercan et al., 1991; Gibaud et al., 1996; Nemmar et al., 2002b, 2003; Hamoir et al., 2003; Silva et al., 2005; Kato et al., 2003; Gibaud et al., 1994, 1998). We implemented the simple way of ^{14}C-styrene synthesis from ^{14}C-methanol with high yield, followed by emulsion polymerization with ^{14}C-PS beads production. Then ^{14}C-aerosol was obtained and tested on mice in low-dose inhalation. To detect ultra-low doses of ^{14}C in different organs we used an accelerator mass-spectrometer (AMS) (Rastigeev et al., 2014).

2. Materials and methods

2.1. Experimental line

The overall experimental process consisted in six steps (Fig. 1): 1) synthesis of ^{14}C-labeled styrene from $^{14}CH_3OH$, 2) emulsion polymerization of ^{14}C-labeled styrene to form PS latex containing radiocarbon in polymeric chain, 3) aerosol generation by pneumatic spraying of diluted ^{14}C-PS latex and aerosol testing on mice for 30 min, 5 days, 4) removal of organs from mice at specified moment of time followed by freezing and keeping in liquid nitrogen, 5) graphitization of probes, and 6) carbon isotope analyses of produced graphite powders. A more detailed description of the steps are below.

2.2. Preparation of polystyrene beads

Polystyrene beads containing radiocarbon ^{14}C label were prepared in five stages (Fig. 2). As a source of radiocarbon label methyl alcohol $^{14}CH_3OH$ (radiochemical purity 98%, JSC Isotope) with activity 40 MBq was chosen.

Synthesis of methyl p-toluenesulfonate from methanol was carried out in the stage I (Fig. 2). At the first step, 5 mL of methyl alcohol $^{14}CH_3OH$ with activity 40 MBq, diluted with 43 mL of common methyl alcohol $^{12}CH_3OH$ (>99%, Acros Organics) and was added to the 225.6 g of p-toluenesulfonyl chloride (99%, Acros Organics). Then 70 mL of 25% sodium hydroxide solution (99%, "Reakhim") was added to the reaction mixture through a dropping funnel while maintaining temperature 23–27 °C. The reaction took place within 4 h. The reaction mixture was placed in a separatory funnel and washed with distilled water. For complete purification methyl p-toluenesulfonate was distilled in vacuum at 10 torr (b.p. 29 °C). Synthesis of iodomethane $^{14}CH_3I$ was carried out in the stage II by the following way. 42.7 g of methyl p-toluenesulfonate was slowly added to the solution of 34.4 g sodium iodide in 53 mL of water at 70 °C. The forming iodomethane was distilled in a well-cooled flask. The product was dried over calcium chloride, filtered and distilled at 42 °C. Synthesis of 1-phenylethanol was carried out in the stage III: 7.8 mL of $^{14}CH_3I$ was diluted with 43 mL of common (Jones, 1999) CH_3I (99%, Acros Organics) and was used for preparation of a Grignard reagent ($^{14}CH_3MgI$) with 19.6 g of magnesium in 300 mL of absolute diethyl ether. Solution of 83.2 mL of freshly distilled benzaldehyde (99%, Acros Organics) in 100 mL of absolute diethyl ether was slowly added to Grignard reagent ethereal solution. After 1 h reaction mixture was decomposed by addition of ammonium chloride saturated solution (150 mL). Organic layer was separated and successively washed by sodium bisulfite solution and water. After drying over $MgSO_4$, ether was distilled under reduced pressure and residue was distilled in vacuum at 4 torr and 71 °C. Styrene was produced in the stage IV. 0.016 g of picric acid and 8.08 mg of p-toluene sulfonic acid was added to the 42.2 mL of 1-phenyl ethanol. Resulting mixture was heated up to 70 °C in vacuum (100 torr). The forming styrene and water were distilled in these conditions. Distillate was dissolved in diethyl ether and dried over magnesium sulfate, and then distilled in vacuum at 60 torr (b.p. 63 °C).

Polymerization of styrene containing radiocarbon label was carried out in the stage V. Emulsion polymerization of styrene was conducted in a thermostated reactor at 90 °C, fitted with a reflux condenser. As initiator of the polymerization $8 \cdot 10^{-3}$ M solution of potassium persulphate (99%, Acros Organics) was used. The volume ratio of styrene to water in the reactor was 1:12.5. Polymerization was conducted for 12 h under continuous flow of nitrogen and magnetic stirring. The diameter (Stokes diameter) of the PS beads in aqueous latex was determined by Malvern Zetasizer Nano ZS based on dynamic light scattering data. Latex concentration, measured by weighting of dried latex aliquots, was 2.5 wt%.

2.3. Aerosol experiments

The scheme of inhalation included an aerosol generator, chambers for mice, filters, diluter, flow control equipment, and aerosol spectrometer (Fig. 3). Aerosol particles were obtained by pneumatic spraying of 150 μL of polystyrene latex diluted in 60 mL of distilled water. The aerosol flow was mixed with the pre-purified air flow and admitted into the nose-only exposure (NOE) glass chambers for mice.

The aerosol camera contained six compartments in which laboratory mice were located. NOE chambers were used to minimize the skin or fur effect. These chambers are constructed so that only the nose was located in the flow of aerosol. The aerosol flow rate was about 50 cm^3 sec^{-1} (Dockery et al., 1992). The aerosol concentration and size distribution were measured with the aerosol spectrometer designed and built at the Institute of Chemical Kinetics and Combustion, Novosibirsk, Russia (Ankilov et al., 2002). This aerosol spectrometer consists of an automatic diffusion battery, condensation chamber, and photoelectric counter. The spectrometer measured the aerosol number concentration and particle

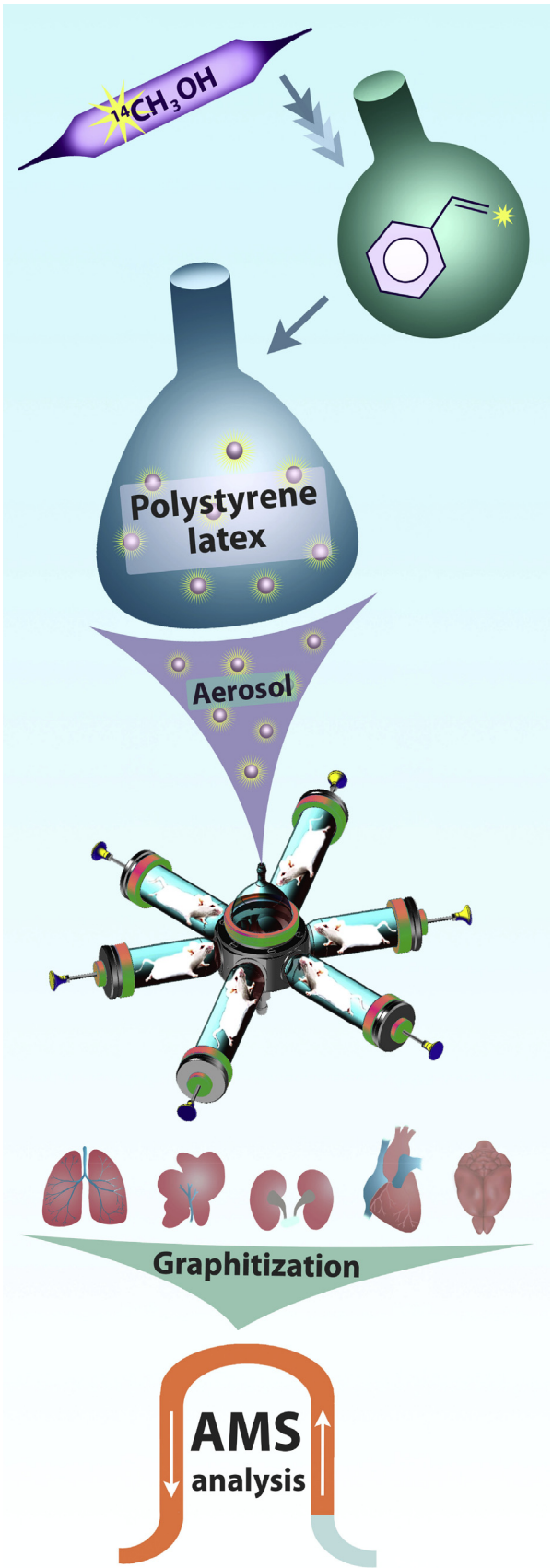

Fig. 1. Experimental line: multistep synthesis of ^{14}C-styrene from ^{14}C-methanol; producing of ^{14}C-PS latex by emulsion polymerization of ^{14}C-styrene; pneumatic spraying of ^{14}C-PS latex for aerosol generation and PM exposure on mice; organ removal from exposured and control mice; organ probe graphitization; AMS carbon isotope analyses of graphite powders.

size distribution at the chamber outlet during the exposure.

The measurement of the concentration and aerosol particles sizes was performed using electron microscopy. The aerosol particles were precipitated onto the films using Thermophoretic Precipitator (Gonzalez et al., 2005) for 20 min at the rate of 1 cm^3 s^{-1}. Then the films with aerosol particles were viewed with a scanning electron microscope. Some few particles were coalesced.

The studies were conducted on male mice of the strain CBA. Animals were housed in cages under a 12 h light regime and free access to food and water. Mice were fed by commercial briquette "ProCorm" (Company BioPro) for laboratory rats and mice, granules d = 11 mm. Before experiments mice passed quarantine and acclimatization within 7 days. Conditions of keeping animals excluded influence of the external factors capable to affect quality of the received results. Air, a forage, water also did not support toxic agents. The inhalation time of tested mice was 30 min once a day for 5 days from March 2nd–6th 2015, then mice were not exposured to PS aerosol. The mice weight was 34.8–35.7 g. Control mice weight was 29.3–29.9 g.

2.4. Preparation of biological samples

Three mice were sacrificed on the fifth day of exposure – March 6th, and then three mice – on each the fourth (March 10th), seventh (March 13th) and fourteenth (March 20th) days postexposure. Lung, liver, heart, brain, and kidney were removed for analysis by AMS. Biological samples were kept at the liquid nitrogen temperature prior to AMS analyses. A simplified way of tissue probe graphitization was implemented in the joint Laboratory of radiocarbon methods of analyses (LRMA) between Novosibirsk State University and Institutes of Russian Academy of Sciences for the further isotopic analyses. 25–35 mg of the mice tissue were detached from each organ and burned in oxygen in the presence of the catalyst Pt/Al_2O_3 at 850 °C. Formed carbon dioxide unlike other gases was adsorbed on calcium oxide at 550 °C, then the sorbent was vacuumed and heated to 920 °C for desorption. Desorbed carbon dioxide was freezed in the cuvette with 6 mg of α-Fe powder (Aldrich-325 mesh) by placing the cuvette to the liquid nitrogen. An appropriate amount of hydrogen was added to the cuvette, then it was heated to 560 °C in the presence of dehumidifier, $Mg(ClO_4)_2$, and kept until the deduction of CO_2 to elementary carbon finished. Then iron-carbon powder, containing 2–3 mg of C, was pressed to tablets, which were subjected to the AMS analyses.

2.5. Radiocarbon analysis

AMS is an ultrasensitive method for measuring isotope ratios. The total radiocarbon content in the graphitized samples was quantified by AMS built by Budker Institute of Nuclear Physics, Novosibirsk, Russia. The radiocarbon atoms can be detected at parts per 10^{15} ^{12}C atoms in milligram samples. The statistical error of measurements for modern samples is smaller than 1%. The total ^{14}C content was measured relative to ^{13}C and normalized to laboratory internal standards: lignin (Aldrich 370959, alkali, $^{14}C/^{13}C = 1.20$) and citric acid (chemical grade, "Reakhim", $^{14}C/^{13}C = 1.00$), which in turn were primarily normalized to NIST oxalic acid I (OxI) and SRM 4990C (OxII). In this way, we usually conserve AMS standards during analyses of hundreds of probes coming from aerosol experiments. It was perfectly acceptable in the work as since in our experiments the ^{14}C-label content was obtained from total ^{14}C

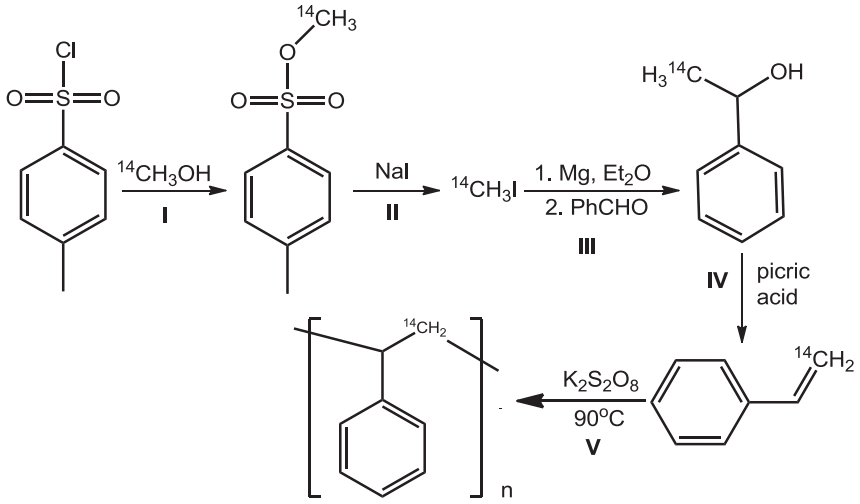

Fig. 2. Five-stage procedure of ^{14}C-PS latex preparation from ^{14}C-methanol.

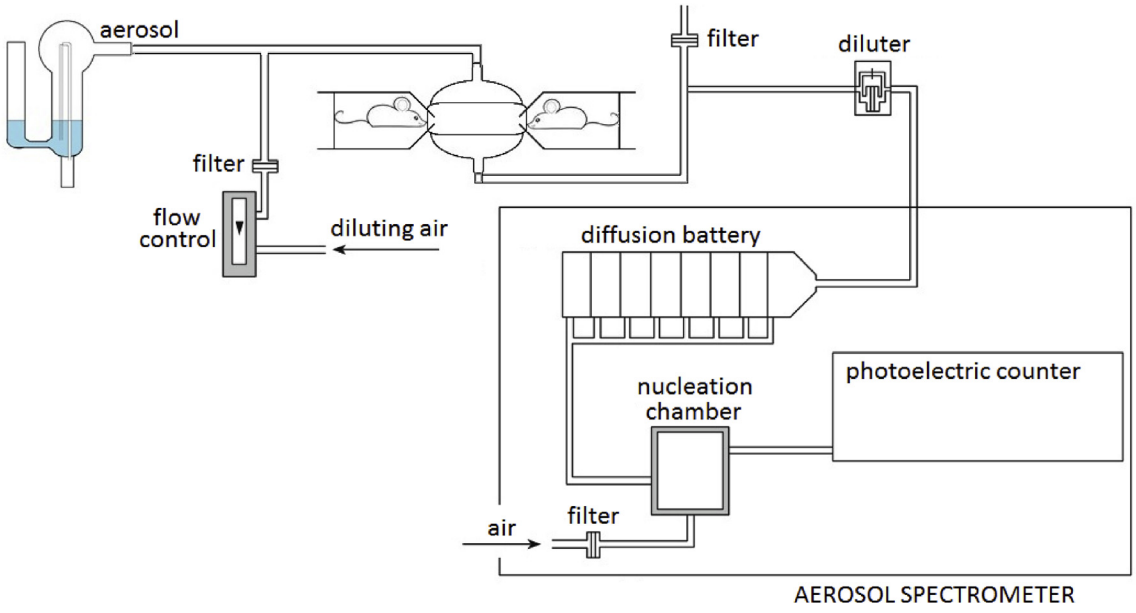

Fig. 3. Scheme of the experimental aerosol setup.

content by normalization to mean value of control mice samples with subtraction. Probes for AMS analyses from control and exposured mice were produced at the same time and conditions. As a result a mean excess of ^{14}C content in organs of exposured mice were calculated according to the equation $(^{14}C/^{13}C)^{mean}_{exp}/(^{14}C/^{13}C)^{mean}_{control} - 1$.

Table 2
Product yields reached during five-step procedure for ^{14}C-PS latex synthesis.

Synthesis stage	Product	Yield, %
I	p-toluenesulfonic acid methyl ester	58.8
II	Iodomethane	58.0
III	1-phenylethanol	38.0
IV	Styrene	47.0
V	Polystyrene	50.0

3. Results and discussion

Reaction yields in each step of ^{14}C-styrene synthesis followed by polymerization (Fig. 2) is indicated in Table 2.

Energy of β-particles produced by the decay of carbon ^{14}C was not sufficient to initiate a spontaneous polymerization reaction due to the activation energy of the reaction being 80.6–97.1 kJ mol^{-1} (Jones, 1999), therefore we used the same conditions for emulsion polymerization of styrene as for unlabeled latex: the absence of emulsifier and β-particle traps, the same temperature and the same ratio of water:styrene. It means that unlabeled latex had the same characteristics as ^{14}C-latex produced at the same conditions described above. The reaction was tested for two times with unlabeled styrene prior to working with radioactivity. The activity of polystyrene latex, measured by scintillation method, was 14 ± 2 kBq/mL, polymer content was 2.5 wt%. According to light scattering data, the polystyrene beads were 225 ± 25 nm in diameter (Fig. 4,a).

The electron microscopy of the dried samples of aerosol

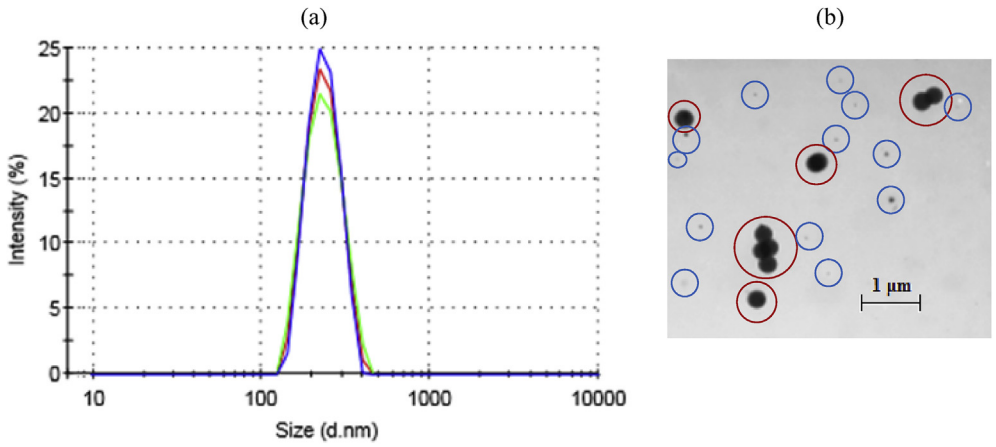

Fig. 4. Distribution of particle sizes of the ^{14}C-PS latex measured three times (green, red and blue curves) by laser light scattering (a) and SEM image of aerosol particles showing 25-nm (blue circles) and 225-nm particles (red circles) (b). (For interpretation of the references to colour in this figure legend, the reader is referred to the web version of this article.)

revealed that polystyrene beads were bidispersed with estimated concentration of 10^3 225-nm particles in cm^3 and $5{\cdot}10^3$ 25-nm particles in cm^3 of aerosol, the procedure of measurement is described in Methods and one of the image is presented in Fig. 4b. The light scattering function of 25-nm particles could be hidden by more massive 225-nm PS particles, that is why we did not observe them in latex by laser scattering method. Despite the fact that 25-nm particles were fivefold abundant in latex its contribution to ^{14}C-content may not be taken into account due to its thousand fold less weight compared with 225-nm PS particles. From SEM analyses the

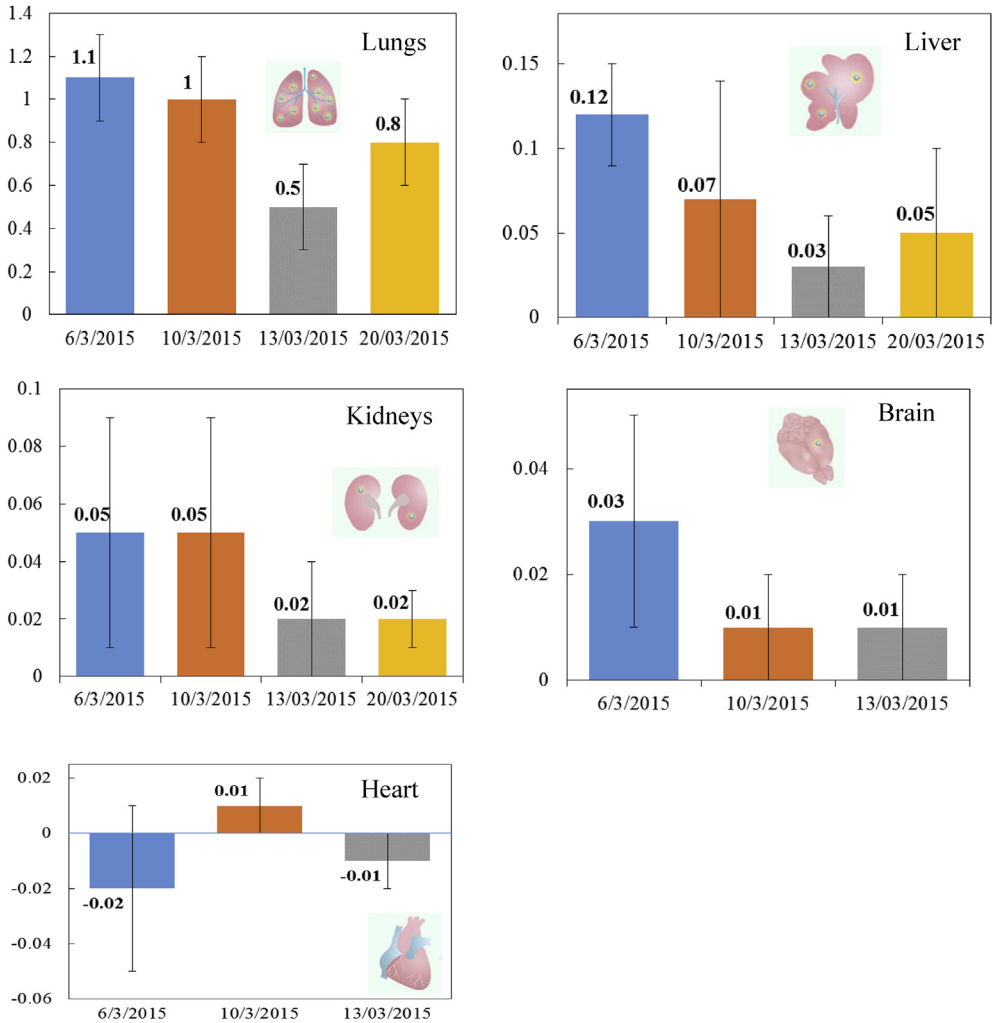

Fig. 5. Mean excess of ^{14}C content in organs of exposured mice over that one of control mice in units of ^{14}C content in control mice on fifth day of exposure (6/03/2015) and on different days of postexposure.

contribution of particle aggregates were estimated as 85% single particle, 11% groups of two particles and 4% groups of three-four particles.

Fig. 5 presents mean excess of ^{14}C content in organs of exposured mice over that one of control mice in units of ^{14}C content in control mice. If the value was more than its deviation then the value was considered as statistically significant and was termed as a reliable one. It should be noted that AMS experiments deviation was much lower than the difference in results for all tested mice, i.e. the data deviations were determined only by variations of results for different mice. A reliable more than twofold increase in radiocarbon content was observed for lungs on the fifth day of exposure. Two weeks of postexposure were insufficient for complete removal of PS particles from the lungs, resulting to 80%-excess of ^{14}C content. A reliable excess of ^{14}C content was also observed in liver on the fifth day of exposure, which dropped to almost zero during two weeks of postexposure. Samples from kidneys and brains presumably also contained an increased amount of radiocarbon on the fifth day of exposure, but there were no reliable changes of ^{14}C content after the end of aerosol exposure. No significant changes of ^{14}C content were also observed in heart on record. However, we may conclude that, unlike heart, probes from kidneys and brain showed positive mean excess of ^{14}C on all days of postexposure that may mean that these organs contained increased amount of radiocarbon but it was at the limit of the method sensitivity.

Thus, considerable PS particles accumulation was observed for organs, performing the highest protection from infections and airborne nanoparticles, they are in decreasing order: lungs, liver and kidneys. This is one more confirmation that the lungs effectively protect an organism from particles more than 200 nm in size. Surprisingly some of 225-nm particles still penetrated to different organs, but, fortunately, liver and kidneys excreted them in short time. The lowest amount of PS particles was in brain possibly due to the blood brain barrier, PM could also penetrate to it not only through the blood system but also through optic nerve via eyes, but this version needs more accurate study. No particles were registered in heart due to high blood flow with low particle concentration through the organ that in addition shows no filtering function.

According to the initial activity of ^{14}C-PS latex the activity of carbon in PS beads was 600 kBq $g_{(C)}^{-1}$. It means that mean ^{14}C excess of 1.1 in lungs over the modern carbon with the activity of 0.23 Bq $g_{(C)}^{-1}$ resulted from 0.25 $g_{(C)}^{-1}$additional activity from labeled PS. If the lungs weight was 0.35 g (1%) and the lung carbon weight was approximately 0.09 g (25%), the whole PS activity in lungs was 0.02 Bq. Assuming that PS beads contained 92 wt% of carbon, one may calculate that lungs stored near $3 \cdot 10^{-8}$ $g_{(PS)}$. As since PS beads were bidispersed and the weight of 25-nm particles may not be taken into account due to its negligible value we can assume that additional radiocarbon in organs originated only from 225-nm PS particles. If the density of PS was 1.04 g cm^{-3}, then the weight of a single PS particle was $6 \cdot 10^{-15}$ g. It means that the lungs accumulated $5.8 \cdot 10^{6}$ particles with 225 nm in size. Analogous calculation for liver, weighting 1.13 g and showing 0.12 mean ^{14}C excess, gives $1 \cdot 10^{-8}$ $g_{(PS)}$ or $2 \cdot 10^{6}$ particles. If we consider the inhalation rate of mouse as 200 breaths min^{-1} with lung volume of 0.2 mL, then during the first exposure procedure the mouse inhaled $1.2 \cdot 10^{6}$ particles and after the fifth day of everyday testing it should accumulate $6 \cdot 10^{6}$ 225-nm particles, which is the same order of magnitude as the sum of particles in all analyzed organs.

4. Conclusions

In conclusion, we firstly synthesized radiocarbon labeled PS beads by emulsifier-free emulsion polymerization of ^{14}C-styrene and investigated the penetration of 225-nm particles, inhaled at low dose by mice, to different organs using direct way of particle registration, based on the ultra-sensitive accelerator mass-spectrometer. Several millions of 225-nm particles deposited in the lungs or ca. 90 μg of particle matter per kg of mice weight and slowly excreted from them during two weeks of postexposure. Penetration of the particles matter was also observed for liver (ca. 17 μg of particle matter per kg of mice weight), kidneys and brain, but not for a heart. A brief evaluation showed that the presented way of aerosol investigation using AMS analyses allowed us to directly register as small as 10^{-8} g of PS beads in 1 g of mice organ, which were inhaled by natural way.

The presented way of aerosol effect investigation allows studying all kinds of organic aerosols, regardless of reactivity and water solubility, if a researcher could synthesize ^{14}C-labeled compounds similar to atmospheric aerosols. Using ^{14}C-labeled polymeric beads, it is especially valuable when studying the effect of size and chemical nature of the surface on the distribution and excretion of inert aerosol particles, inhaled by natural way.

Acknowledgements

The authors are grateful to I.A. Pyshnaya for the opportunity to analyze the polystyrene beads on the Zeta Sizer Nano, V.V. Sukulova for polystyrene activity determination, M.A. Kuleshova, D.V. Kuleshov and A.V. Petrozhitsky for mice probe preparation for AMS analyses.

References

Ankilov, A., Baklanov, A., Colhoun, M., Enderle, K.-H., Gras, J., Yu, Junlanov, Kaller, D., Lindner, A., Lushnikov, A.A., Mavliev, R., McGovern, F., Mirme, A., O'Connor, T.C., Podzimek, J., Preining, O., Reischl, G.P., Rudolf, R., Sem, G.J., Szymanski, W.W., Tamm, E., Vrtala, A.E., Wagner, P.E., Winklmayr, W., Zagaynov, V., 2002. Intercomparison of number concentration measurements by various aerosol particle counters. Atmos. Res. 62, 177–207.

Bascom, R., Bromberg, P.A., Costa, D.A., Devlin, R., Dockery, D.W., Frampton, M.W., Lambert, W., Samet, J.M., Speizer, F.E., Utell, M., 1996. Health effects of outdoor air pollution. Am. J. Respir. Crit. Care Med. 153 (1), 3–50.

Bernstein, J.A., Alexis, N., Barnes, C., Bernstein, I.L., Bernstein, J.A., Nel, A., Peden, D., Diaz-Sanchez, D., Tarlo, S.M., Williams, P.B., 2004. Health effects of air pollution. J. Allergy Clin. Immunol. 114 (5), 1116–1123.

Brunekreef, B., Holgate, S.T., 2002. Air pollution and health. Lancet 360 (9341), 1233–1242.

Cohen, A.J., Anderson, H.R., Ostro, B., Pandey, K.D., Krzyzanowski, M., Künzli, N., Gutschmidt, K., Pope, A., Romieu, I., Samet, J.M., Smith, K., 9 July 2005. The global burden of disease due to outdoor air pollution. J. Toxicol. Environ. Health Part A 68 (13–14), 1301–1307.

Conhaim, R.L., Eaton, A., Staub, N.C., Heath, T.D., 1988. Equivalent pore estimate for the alveolar-airway barrier in isolated dog lung. J. Appl. Physiol. 64 (3), 1134–1142.

Dockery, D.W., Speizer, F.E., Stram, D.O., Ware, J.H., Spengler, J.D., Ferris Jr., B.G., 1989. Effects of inhalable particles on respiratory health of children. Am. Rev. Respir. Dis. 139 (3), 587–594.

Dockery, D.W., Schwartz, J., Spengler, J.D., 1992. Air pollution and daily mortality: associations with particulates and acid aerosols. Environ. Res. 59 (2), 362–373.

Donaldson, K., Li, X.Y., MacNee, W., 1998. Ultrafine (nanometre) particle mediated lung injury. J. Aerosol Sci. 29 (5–6), 553–560.

Ercan, M.T., Tuncel, S.A., Caner, B.E., Mutlu, M., Pikin, E., 1991. Evaluation of 99mTc labelled monodisperse polystyrene/polyacrylate latex Ps for the study of colon transit and morphology. Int. J. Radiat. Appl. Instrum. 18 (2), 253–258.

Ferin, J., Oberdörster, G., Penney, D.P., 1992. Pulmonary retention of ultrafine and fine Ps in rats. Am. J. Respir Cell Mol. Biol. 6 (5), 535–542.

Geiser, M., Rothen-Rutishauser, B., Kapp, N., Schürch, S., Kreyling, W., Schulz, H., Semmler, M., Im Hof, V., Heyder, J., Gehr, P., 2005. Ultrafine Ps cross cellular membranes by nonphagocytic mechanisms in lungs and in cultured cells. Environ. Health Perspect. 113 (11), 1555–1560.

Gibaud, S., Andreux, J.P., Weingarten, C., Renard, M., Couvreur, P., 1994. Increased bone marrow toxicity of doxorubicin bound to nanoPs. Eur. J. Cancer 30 (6), 820–826.

Gibaud, S., Demoy, M., Andreux, J.P., Weingarten, C., Gouritin, B., Couvreur, P., 1996. Cells involved in the capture of nanoPs in hematopoietic organs. J. Pharm. Sci. 85 (9), 944–950.

Gibaud, S., Rousseau, C., Weingarten, C., Favier, R., Douay, L., Andreux, J.P., Couvreur, P., 1998. Polyalkylcyanoacrylate nanoPs as carriers for granulocyte

colony stimulating factor (G-CSF). J. Control. Release 52 (1–2), 131–139.
Glover, W., Chan, H.-K., Eberl, S., Daviskas, E., Verschuer, J., 2008. Effect of P size of dry powder mannitol on the lung deposition in healthy volunteers. Int. J. Pharm. 349 (1–2), 314–322.
Gonzalez, D., Nasibulin, A.G., Baklanov, A.M., Shandakov, S.D., Brown, D.P., Queipo, P., Kauppinen, E.I., 2005. A new thermophoretic precipitator for collection of nanometer-sized aerosol particles. Aerosol Sci. Technol. 39 (11), 1064–1071.
Hamoir, J., Nemmar, A., Halloy, D., Wirth, D., Vincke, G., Vanderplasschen, A., Nemery, B., Gustin, P., 2003. Toxicol. Appl. Pharmacol. 190 (3), 278–285.
Jones, A.P., 1999. Indoor air quality and health. Atmos. Environ. 33 (28), 4535–4564.
Kato, T., Yashiro, T., Murata, Y., Herbert, D.C., Oshikawa, K., Bando, M., Ohno, S., Sugiyama, Y., 2003. Evidence that exogenous substances can be phagocytized by alveolar epithelial cells and transported into blood capillaries. Cell Tissue Res. 311 (1), 47–51.
Khorasanizade, S., Shams, M., Mansoori, B.M., 2011. Calculation of aerosol deposition in human lung airways using Horsfield geometric model. Adv. Powder Technol. 22 (6), 695–705.
Künzli, N., Kaiser, R., Medina, S., Studnicka, M., Chanel, O., Filliger, P., Herry, M., Horak Jr., F., Puybonnieux-Texier, V., Quénel, P., Schneider, J., Seethaler, R., Vergnaud, J.-C., Sommer, H., 2000. Public-health impact of outdoor and traffic-related air pollution: a European assessment. Lancet 356 (9232), 795–801.
Li, N., Sioutas, C., Cho, A., Schmitz, D., Misra, C., Sempf, J., Wang, M., Oberley, T., Froines, J., Nel, A., 2003. Ultrafine particulate pollutants induce oxidative stress and mitochondrial damage. Environ. Health Perspect. 111 (4), 455–460.
Lumley, Th, Sheppard, L., 2003. Time series analyses of air pollution and health: straining at gnats and swallowing camels? Epidemiology 14 (1), 13–14.
Mauderly, J.L., Chow, J.C., 2008. Health effects of organic aerosols. Inhal. Toxicol. 20 (3), 257–288.
Miller, F.J., Gardner, D.E., Graham, J.A., 1979. Size considerations for establishing a standard for inhalable particles. J. Air Pollut. Control Assoc. 29 (6), 610–615.
Nel, A., 2005. Air pollution-related illness: effects of particles. Science 308 (5723), 804–806.
Nemmar, A., Vanbilloen, H., Hoylaerts, M.F., Hoet, P.H.M., Verbruggen, A., Nemery, B., 2001. Passage of intratracheally instilled ultrafine Ps from the lung into the systemic circulation in hamster. Am. J. Respir. Crit. Care Med. 164 (9), 1665–1668.
Nemmar, A., Hoet, P.H.M., Vanquickenborne, B., Dinsdale, D., Thomeer, M., Hoylaerts, M.F., Vanbilloen, H., Mortelmans, L., Nemery, B., 2002. Passage of inhaled Ps into the blood circulation in humans. Circulation 105 (4), 411–414.
Nemmar, A., Hoylaerts, M.F., Hoet, P.H.M., Dinsdale, D., Smith, T., Xu, H., Vermylen, J., Nemery, B., 2002. Ultrafine Ps affect experimental thrombosis in an in vivo hamster model. Am. J. Respir. Crit. Care Med. 166 (7), 998–1004.
Nemmar, A., Hoylaerts, M.F., Hoet, P.H.M., Vermylen, J., Nemery, B., 2003. Size effect of intratracheally instilled particles on pulmonary inflammation and vascular thrombosis. Toxicol. Appl. Pharmacol. 186 (1), 38–45.
Oberdörster, G., 2001. Pulmonary effects of inhaled ultrafine particles. Int. Archives Occup. Environ. Health 74 (1), 1–8.
Oberdörster, G., 2001. Pulmonary effects of inhaled ultrafine Ps. Int. Archives Occup. Environ. Health 74 (1), 1–8.
Oberdörster, G., Ferin, J., Morrow, P.E., 1992. Volumetric loading of alveolar macrophages (AM): a possible basis for diminished AM-mediated P clearance. Exp. Lung Res. 18 (1), 87–104.
Oberdorster, G., Ferin, J., Lehnert, B.E., 1994. Correlation between P size, in vivo P persistence, and lung injury. Environ. Health Perspect. 102 (Suppl. 5), 173–179.
Oberdörster, G., Sharp, Z., Atudorei, V., Elder, A., Gelein, R., Lunts, A., Kreyling, W., Cox, C., 2002. Extrapulmonary translocation of ultrafine carbon particles following whole-body inhalation exposure of rats. J.Toxic. Environ. Health Part A 65 (20), 1531–1543.
Oberdörster, G., Sharp, Z., Atudorei, V., Elder, A., Gelein, R., Lunts, A., Kreyling, W., Cox, C., 2002. Extrapulmonary translocation of ultrafine carbon Ps following whole-body inhalation exposure of rats. J.Toxic. Environ. Health Part A 65 (20), 1531–1543.
Oberdörster, G., Sharp, Z., Atudorei, V., Elder, A., Gelein, R., Kreyling, W., Cox, C., 2004. Translocation of inhaled ultrafine particles to the brain. Inhal. Toxicol. 16 (6–7), 437–445.
Oberdörster, G., Oberdörster, E., Oberdörster, J., 2005. Nanotoxicology: an emerging discipline evolving from studies of ultrafine particles. Environ. Health Perspect. 113 (7), 823–839.
Peters, A., Döring, A., Wichmann, H.-E., Koenig, W., 1997. Increased plasma viscosity during an air pollution episode: a link to mortality? Lancet 349 (9065), 1582–1587.
Peters, A., Wichmann, H.E., Tuch, T., Heinrich, J., Heyder, J., 1997. Respiratory effects are associated with the number of ultrafine particles. Am. J. Respir. Crit. Care Med. 155 (4), 1376–1383.
Pope III, C.A., Dockery, D.W., 2006. Health effects of fine particulate air pollution: lines that connect. J. Air Waste Manag. Assoc. 56 (6), 709–742.
Pope III, C.A., Schwartz, J., Ransom, M.R., 1992. Daily mortality and PM10 pollution in Utah Valley. Archives Environ. Health 47 (3), 211–217.
Rastigeev, S.A., Frolov, A.R., Goncharov, A.D., Klyuev, V.F., Konstantinov, E.S., Kutnyakova, L.A., Parkhomchuk, V.V., Petrozhitskii, A.V., 2014. Acceleration mass spectrometer of the budker Institute of nuclear Physics for biomedical applications. Phys. Part. Nucl. Lett. 11 (5), 642–646.
Samet, J.M., Dominici, F., Curriero, F.C., Coursac, I., Zeger, S.L., 2000. Fine particulate air pollution and mortality in 20 U.S. cities, 1987-1994. N. Engl. J. Med. 343 (24), 1742–1749.
Schwartz, J., 1994. Air pollution and daily mortality: a review and meta analysis. Environ. Res. 64 (1), 36–52.
Schwartz, J., Dockery, D.W., Neas, L.M., 1996. Is daily mortality associated specifically with fine particles? J. Air Waste Manag. Assoc. 46 (10), 927–939.
Silva, V.M., Corson, N., Elder, A., Oberdörster, G., 2005. The rat ear vein model for investigating in vivo thrombogenicity of ultrafine Ps (UFP). Toxicol. Sci. 85 (2), 983–989.
Simon, B.H., Ando, H.Y., Gupta, P.K., 1995. Circulation time and body distribution of 14C-labeled amino-modified polystyrene nanoPs in mice. J. Pharm. Sci. 84 (10), 1249–1253.
Simon, B.H., Ando, H.Y., Gupta, P.K., 1995. Circulation time and body distribution of protein A-coated amino modified polystyrene nanoparticles in mice. Int. J. Pharm. 121 (2), 233–237.
Takenaka, S., Karg, E., Roth, C., Schulz, H., Ziesenis, A., Heinzmann, U., Schramel, P., Heyder, J., 2001. Pulmonary and systemic distribution of inhaled ultrafine silver Ps in rats. Environ. Health Perspect. 109 (Suppl. 4), 547–551.
Wallace, L., 1996. Indoor particles: a review. J. Air Waste Manag. Assoc. 46 (2), 98–126.
Ware, J.H., 2000. Particulate air pollution and mortality – clearing the air. N. Engl. J. Med. 343 (24), 1798–1799.
Williams III, R.O., Carvalho, T.C., Peters, J.I., 2011. Influence of particle size on regional lung deposition – what evidence is there? Int. J. Pharm. 406 (1–2), 1–10.
Wilson, W.E., Suh, H.H., 1997. Fine particles and coarse particles: concentration relationships relevant to epidemiologic studies. J. Air Waste Manag. Assoc. 47 (12), 1238–1249.